

Dynamic behaviour of high-sided road vehicles subject to a sudden crosswind gust

Y.L. Xu[†]

*Department of Civil and Structural Engineering, The Hong Kong Polytechnic University,
Hung Hom, Kowloon, Hong Kong*

W.H. Guo[‡]

*School of Civil Engineering and Architecture, Central South University, Changsha, China
(Received February 17, 2003, Accepted October 11, 2003)*

Abstract. High-sided road vehicles are susceptible to a sharp-edged crosswind gust, which may cause vehicle accidents such as overturning, excessive sideslip, or exaggerated rotation. This paper thus investigates the dynamic behaviour and possible accidents of high-sided road vehicles entering a sharp-edged crosswind gust with road surface roughness and vehicle suspension included. The high-sided road vehicle is modelled as a combination of several rigid bodies connected by a series of springs and dampers in both vertical and lateral directions. The random roughness of road surface is generated from power spectral density functions for various road conditions. The empirical formulae derived from wind tunnel test results are employed to determine aerodynamic forces and moments acting on the vehicle. After the governing equations of motion are established, an extensive computation work is performed to examine the effects of road surface roughness and vehicle suspension on the dynamic behaviour and vehicle accidents. It is demonstrated that for the high-sided road vehicle and wind forces specified in the computation, the accident vehicle speed of the road vehicle running on the road of average condition is relatively smaller than that running on the road of very good condition for a given crosswind gust. The vehicle suspension system should be taken into consideration, and the accident vehicle speed becomes smaller if the vehicle suspension system has softer springs and lighter dampers.

Keywords: high-sided road vehicle; crosswind gust; dynamic behaviour; vehicle accidents; road roughness; vehicle suspension.

1. Introduction

Wind induced accidents of road vehicles of various types have become a topic of increasing concern in recent years. This is because not only vehicle volumes are dramatically increased, but also vehicle weights are significantly reduced owing to the use of more efficient structural design and lighter weight materials. Baker and Reynolds (1992) carried out a post-disaster investigation on wind-induced vehicle accidents that occurred in the United Kingdom during the major storm of 25

[†] Chair Professor

[‡] Associate Professor

January 1990. They found that among 400 wind-induced vehicle accidents in that event, overturning accidents were the most common type of wind-induced accident, accounting for 47% of the total. Course deviation accidents made up 19% of the total. Sixty-six percent of the accidents involved high-sided lorries or vans whilst only 27% involved cars. Pritchard (1985) carried out an investigation of wind effects on high-sided road vehicles running over long span cable-supported bridges. He pointed out that vehicle speed limits should be imposed when the wind blew across the bridge. The reason for this is that as high-sided vehicles pass the bridge towers, they are briefly shielded from the wind but when they pass out of the shelter of the tower, they enter a sharp-edged crosswind gust with the obvious danger of turning them over. To this end, this paper focuses on the dynamic behaviour and possible accidents of high-sided road vehicles subject to a sudden crosswind gust.

Baker and his colleagues have conducted a systematic study on the concerned subject. Baker (1986) developed a theoretical model that described the dynamics of vehicles in crosswind. Coleman and Baker (1990) performed a series of wind tunnel tests to determine the aerodynamic forces and moments on road vehicles of certain types. Baker (1987) then quantified accident wind speeds of road vehicles for overturning, sideslip, and rotation accidents and estimated accident risk. However, when they calibrated their framework and the associated computer program against the full scale vehicle accident data collected from the major storm event of 25 January 1990 in the United Kingdom, they found that the computed accident wind speeds based on their framework were perhaps rather too high. They attributed this discrepancy to the lack of reliable aerodynamic force and moment coefficient data for vehicles. Though further experimental investigations should be performed to gain reliable aerodynamic force and moment coefficients, it may be also necessary to pay a revisit of their theoretical model. This is because their framework is based on a single-mass vehicle system under the action of its own weight, tyre forces and aerodynamic forces and moments. The vehicle suspension and the variation of centre of gravity position of the vehicle with respect to the tyre contact points were not considered in their model. Moreover, the road surface roughness, which is an important factor that affects dynamics of road vehicles, was not taken into consideration in their model. The vertical acceleration of the vehicle was also assumed zero in their model, which may affect tyre contact forces and accident wind speeds.

In this connection, this paper presents a refined dynamic model of high-sided road vehicles subject to a sudden crosswind gust. A more realistic and rational vehicle model is developed using a combination of several rigid bodies connected by a series of springs and dampers in both vertical and lateral directions. The road surface roughness is included and generated from power spectral density functions for various road conditions. The empirical formulae are employed to determine aerodynamic forces and moments acting on the vehicle. The equations of motion of high-sided road vehicles under a sudden crosswind gust are then derived and solved by the direct integration method. An extensive computation work is finally performed for a typical high-sided road vehicle with emphasis on the effects of road surface roughness and vehicle suspension on vehicle accidents.

2. Wind-induced vehicle accidents

Post-disaster investigations of wind-induced vehicle accidents reveal that the most severe condition that a vehicle accident may occur is when the vehicle encounters a sharp-edged crosswind gust. Under such a situation, the vehicle may be turned over, or it may be blown a significant distance sideways, or it may rotate through a significant angle. Thus, Baker (1987) suggested that a

wind-induced vehicle accident was said to occur if, within 0.5s of the vehicle entering a sharp-edged crosswind gust, one of the tyre reactions fell to zero (an overturning accident), or the lateral displacement exceeded 0.5 m (a sideslip accident), or the rotational displacement exceeded 0.2 radians (a rotational accident). The accident vehicle speed at which any one of the three accident criteria is first exceeded can be thus found. However, it should be pointed out that the above definition is conservative in several aspects. Firstly, it was assumed that within the 0.5 second the driver of the vehicle would not react to correct any lateral or rotational displacement. Secondly, a sharp-edged crosswind gust was assumed. Thirdly, the aerodynamic force coefficients were assumed to be constant within the 0.5 second. Nevertheless, this study is mainly a comparison study in finding the effects of road roughness and vehicle suspension on accident vehicle speed. The definition of vehicle accidents given above is acceptable.

3. Modelling of road vehicle and surface roughness

3.1. Modelling of high-sided road vehicle

In this study, not only the vertical vibration but also the lateral and rotational vibrations of a high-sided road vehicle are considered in order to investigate the course deviation of vehicle caused by a sudden crosswind gust. A high-sided road vehicle is modelled as a combination of several rigid bodies connected by a series of springs, dampers, and pivots (see Fig. 1) so that the effects of vehicle suspension on vehicle accidents can be investigated. The rigid bodies are used to represent the vehicle bodies, the axles, the wheels, or others. The centre of gravity of each rigid body is taken as a node, which has six degrees of freedom in general: three translational degrees and three rotational degrees with respect to the local co-ordinate originated at the node. The displacements and rotations of the vehicle body and axles are assumed to remain small throughout the analysis so that the sines of the angles of rotation may be taken equal to angles themselves and the cosines of the angles of rotation may be taken as unity, leading to linear equations of motion for the vehicle itself (Fafard, *et al.* 1997). The mass and/or the mass moments of inertia of each rigid body are

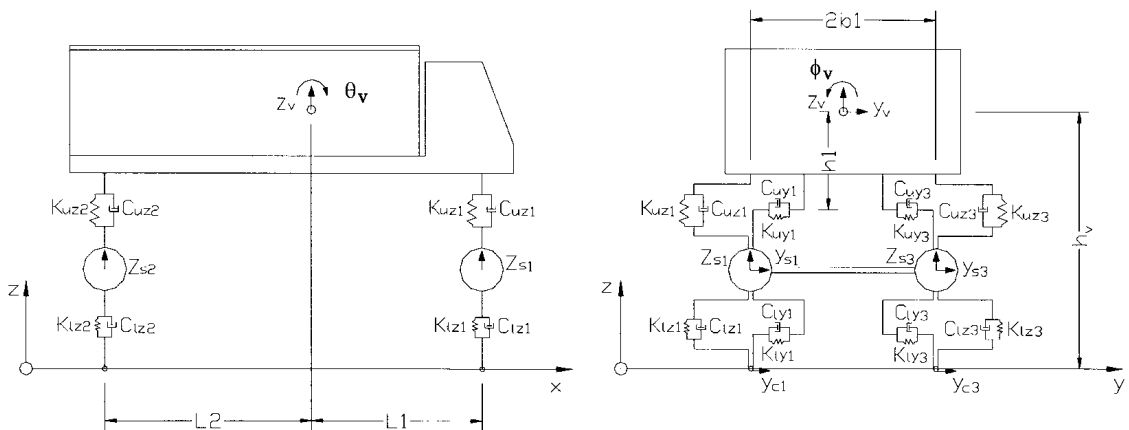


Fig. 1 Vehicle model used in case study

calculated from the weight distribution and dimension of the body with respect to its local co-ordinate.

A vehicle tyre is assumed to be a point in this study, and the contact between the road surface and the vehicle tyre is thus a point contact. The road surface is not too rough to make the vehicle tyre jump or leave the riding surface. The tyres of the vehicle therefore remain in contact with road surface at all times except for the occurrence of overturning of the vehicle, in which the contact force between the road surface and any one of the vehicle tyres becomes zero. As a result, the vertical displacement of the tyre is not an independent degree of freedom and can thus be determined by the vertical road surface profile and its relative position. However, the lateral displacement of the tyre should be taken as an independent degree of freedom because of the vehicle sideslip relative to the road surface.

The springs can be used to model the suspension system, the flexibility of a tyre, or others. Each spring is assumed to be massless. Apart from the stiffness coefficient of each spring, the positions of the two ends of the spring connecting two rigid bodies or connecting one rigid body and one contact point are required as input data. The energy dissipation capacity of the suspension system and the tyres can be modelled by dampers. If the damper is of a viscous type, the damping coefficient can be used as a sole parameter for the damping device. The pivots may be used to connect the trailer to the tractor, for which the constraint equations should be correspondingly developed.

In summary, the input data about road vehicles required by the computer program at a given time are the dynamic properties and positions of all the rigid bodies and the springs and the dampers, the positions of all the contact points, and the constraint conditions for all the pivots. Based on these input data, the mass matrix, the damping matrix, and the stiffness matrix of the vehicle and the force vectors due to road surface roughness can be automatically assembled using a fully computerised approach developed by the writers (Guo and Xu 2001), which will be demonstrated later in this paper.

3.2. Modelling of road surface roughness

Many investigations have shown that the roughness of road surface is an important factor that affects the dynamic response of a vehicle (Wang and Huang 1992). It is thus envisaged that the road surface roughness has also an impact on vehicle accidents. The road surface roughness in the vertical direction may be described as a realisation of a random process that can be described by a power spectral density (PSD) function. The following PSD functions were proposed by Dodds and Robson (1973) for road surface roughness of a highway in the vertical direction:

$$S(\bar{\phi}) = A_r \left(\frac{\bar{\phi}}{\bar{\phi}_0} \right)^{-w_1}, \quad \bar{\phi} \leq \bar{\phi}_0 \quad (1)$$

$$S(\bar{\phi}) = A_r \left(\frac{\bar{\phi}}{\bar{\phi}_0} \right)^{-w_2}, \quad \bar{\phi} \geq \bar{\phi}_0 \quad (2)$$

where $S(\bar{\phi})$ is the PSD function (m^3/cycle) for the road surface roughness in the vertical direction; $\bar{\phi}$ is the spatial frequency (cycle/m); $\bar{\phi}_0$ is the discontinuity frequency of $1/2\pi$ (cycle/m); and A_r is

the roughness coefficient (m^3/cycle) depending on the road condition. The power exponents w_1 and w_2 vary from 1.36 to 2.28. To simplify the description of the road surface roughness, Huang and Wang (1992) suggested the following PSD function.

$$S(\bar{\phi}) = A_r \left(\frac{\bar{\phi}}{\bar{\phi}_0} \right)^{-2} \quad (3)$$

The vertical road surface roughness is assumed to be a periodically modulated random process, and its time-history can be generated through an inverse Fourier transform.

$$r(x) = \sum_{k=1}^N \sqrt{2S(\bar{\phi}_k)\Delta\bar{\phi}} \cos(2\pi\bar{\phi}_k x + \theta_k) \quad (4)$$

where θ_k is the random phase angle uniformly distributed from 0 to 2π . While the road surface roughness in the vertical direction can be modelled, the road surface roughness in the lateral direction cannot be considered at this stage owing to the lack of relevant information.

4. Aerodynamic forces and moments on road vehicle

The aerodynamic forces and moments on the vehicle measured from wind tunnel tests (Coleman and Baker 1990) are used as a sudden crosswind gust without considering aerodynamic weighting function as done in the previous study (Baker 1986). The exclusion of aerodynamic weighting function may lead to conservative accident vehicle speed because the realistic gust speed increases over a period of a few seconds rather than instantaneously, and the force and moment coefficients build up over a short period of time rather than keep constant. Nevertheless, this study is mainly a comparison study in finding the effects of road roughness and vehicle suspension on accident vehicle speed, and the influence of aerodynamic weighting function on the results is expected to be small.

In this study, the wind velocity U_m is assumed to be perpendicular to the longitudinal axis of the road and the road vehicle runs on the road at a constant velocity of U_v . Then, the wind velocity relative to the vehicle, U_R , and its yaw angle Ψ (see Fig. 2(a)) can be expressed as

$$U_R = \sqrt{U_m^2 + U_v^2} \quad (5)$$

$$\Psi = \arctan\left(\frac{U_m}{U_v}\right) \quad (6)$$

The aerodynamic forces and moments acting on the vehicle can then be expressed by

$$F_x = \frac{1}{2}\rho U_R^2 C_D(\Psi) A_f \quad (7)$$

$$F_y = \frac{1}{2}\rho U_R^2 C_S(\Psi) A_f \quad (8)$$

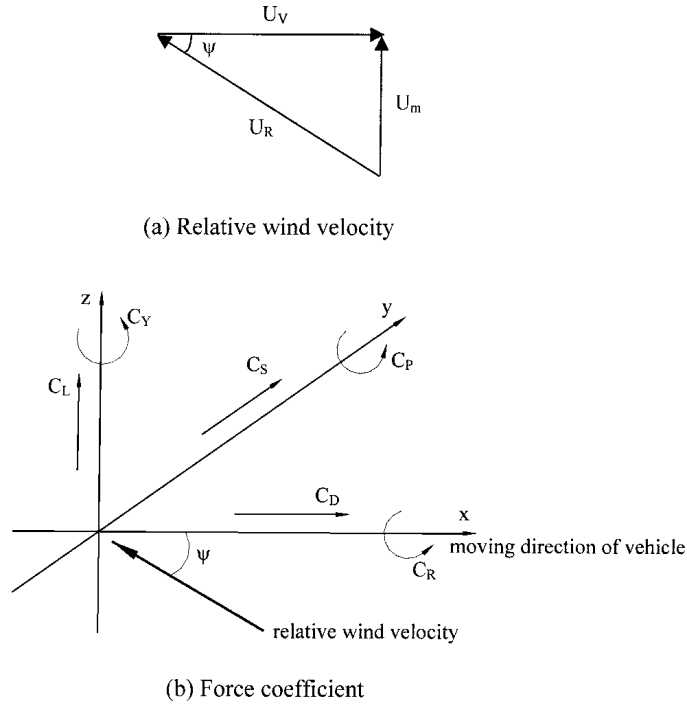


Fig. 2 Sign convention for wind velocities and wind forces

$$F_z = \frac{1}{2} \rho U_R^2 C_L(\psi) A_f \quad (9)$$

$$M_x = \frac{1}{2} \rho U_R^2 C_R(\psi) A_f h_v \quad (10)$$

$$M_y = \frac{1}{2} \rho U_R^2 C_P(\psi) A_f h_v \quad (11)$$

$$M_z = \frac{1}{2} \rho U_R^2 C_Y(\psi) A_f h_v \quad (12)$$

where F_x , F_y , F_z , M_x , M_y , and M_z are the drag force, side force, lift force, rolling moment, pitching moment, and yawing moment acting on the vehicle respectively; $C_D(\psi)$, $C_S(\psi)$, $C_L(\psi)$, $C_R(\psi)$, $C_P(\psi)$, and $C_Y(\psi)$ are the drag force coefficient, side force coefficient, lift force coefficient, rolling moment coefficient, pitching moment coefficient, and yawing moment coefficient, respectively, which are a function of yaw angle Ψ ; A_f is the reference area, which is normally taken as the frontal area of the vehicle; and h_v is the reference height, which is normally taken as the height of the vehicle centre of gravity above the ground as done by Baker (1986). The force and moment coefficients are usually obtained through wind tunnel tests and a sign convention for these coefficients is given in Fig. 2(b).

5. Governing equations of motion of road vehicle

A large truck shown schematically in Fig. 1 is taken as an example to investigate the dynamic behaviour and possible accidents of high-sided road vehicles subject to a sudden crosswind gust in this study. The vehicle comprises 9 rigid bodies: one for the vehicle body, two for the front axle set, two for the rear axle set, and four for the tyres (see Fig. 1). It is assumed that the vehicle runs at a constant velocity on a straight road. Thus, the position of the vehicle in the X -direction can be determined accurately at any given time as long as the initial position of the vehicle is known. In this connection, the degrees of freedom in the X -direction are not included. The vehicle body is assigned five degrees of freedom with respect to its gravity centre: the vertical displacement (Z_v), the lateral displacement (Y_v), the rotation about the Y -axis (pitching angle θ_v), the rotation about the X -axis (rolling angle ϕ_v), and the rotation about the Z -axis (yawing angle φ_v). Each rigid body in either the front axle set or the rear axle set is assigned two degrees of freedom in the Z -direction (Z_{si}) and the Y -direction (Y_{si}). Since the vehicle tyre is assumed to be a pint and have a sideslip, each rigid body for one tyre is assigned one degree of freedom (Y_{ci}) in the Y -direction. As a result, the vehicle concerned has a total of 17 degrees of freedom.

$$\{v_v\} = \{Z_v \ Y_v \ \theta_v \ \phi_v \ \varphi_v \ Z_{s1} \ Y_{s1} \ Z_{s2} \ Y_{s2} \ Z_{s3} \ Y_{s3} \ Z_{s4} \ Y_{s4} \ Y_{c1} \ Y_{c2} \ Y_{c3} \ Y_{c4}\} \quad (13)$$

In Eq. (13), all the vertical displacements of the vehicle are measured from the position of static equilibrium.

Each rigid body in either the front axle set or the rear axle set is connected to the vehicle body through two suspension units: one is the parallel combination of a linear elastic spring of stiffness K_{uzi} and a viscous damper of damping coefficient C_{uzi} in the Z -direction, and the other is the parallel combination of a linear elastic spring of stiffness K_{uyi} and a viscous damper of damping coefficient C_{uyi} in the Y -direction. The connection of each rigid body in either the front axle set or the rear axle set to the tyre is realised through the two units representing the dynamic characteristics of the tyre: one is the parallel combination of a linear elastic spring of stiffness K_{lzi} and a viscous damper of damping coefficient C_{lzi} in the Z -direction and the other is the parallel combination of a linear elastic spring of stiffness K_{lyi} and a viscous damper of damping coefficient C_{lyi} in the Y -direction. The horizontal distance between the two rigid bodies in either the front axle set or the rear axle set is $2b_1$. The other major parameters of the vehicle are listed in Table 1.

The use of the fully computerised approach (Guo and Xu 2001) can easily lead to the equations of motion of the vehicle under a sudden crosswind gust, established from the static equilibrium position of the vehicle. They are given as follows:

The equation of motion of the vehicle body in the Y -direction is

$$\begin{aligned} M_v \ddot{Y}_v + C_{uy1}(\dot{Y}_v + h_1 \dot{\phi}_v + L_1 \dot{\varphi}_v - \dot{Y}_{s1}) + C_{uy2}(\dot{Y}_v + h_1 \dot{\phi}_v - L_2 \dot{\varphi}_v - \dot{Y}_{s2}) + C_{uy3}(\dot{Y}_v + h_1 \dot{\phi}_v + L_1 \dot{\varphi}_v - \dot{Y}_{s3}) \\ + C_{uy4}(\dot{Y}_v + h_1 \dot{\phi}_v - L_2 \dot{\varphi}_v - \dot{Y}_{s4}) + K_{uy1}(Y_v + h_1 \phi_v + L_1 \varphi_v - Y_{s1}) + K_{uy2}(Y_v + h_1 \phi_v - L_2 \varphi_v - Y_{s2}) \\ + K_{uy3}(Y_v + h_1 \phi_v + L_1 \varphi_v - Y_{s3}) + K_{uy4}(Y_v + h_1 \phi_v - L_2 \varphi_v - Y_{s4}) = F_{vyw} \end{aligned} \quad (14)$$

where F_{vyw} is the aerodynamic force acting on the vehicle body in the Y -direction and other parameters can be found in Table 1.

The equation of motion of the vehicle body in the Z -direction is

Table 1 Major parameters of the vehicle used in case study

| Parameter | Unit | Value |
|---|---------------------|--------|
| Full length of vehicle (L) | m | 13.450 |
| Total weight of vehicle (W_v) | kN | 73.575 |
| Mass of truck body (M_v) | kg | 4480 |
| Pitching moment of inertia of truck body (J_{yv}) | kg · m ² | 5516 |
| Rolling moment of inertia of truck body (J_{xv}) | kg · m ² | 1349 |
| Yawing moment of inertia of truck body (J_{zv}) | kg · m ² | 100000 |
| Mass of axle set ($M_{s1}=M_{s3}$) | kg | 800 |
| Mass of axle set ($M_{s2}=M_{s4}$) | kg | 710 |
| Mass of tires ($M_{c1}=M_{c2}=M_{c3}=M_{c4}$) | kg | 0.0 |
| Upper vertical spring stiffness ($K_{uz1}=K_{uz2}=K_{uz3}=K_{uz4}$) | kN/m | 399 |
| Upper lateral spring stiffness ($K_{uy1}=K_{uy2}=K_{uy3}=K_{uy4}$) | kN/m | 299 |
| Upper vertical damper damping coefficient ($C_{uz1}=C_{uz3}$) | kN · s/m | 23.21 |
| Upper lateral damper damping coefficient ($C_{uy1}=C_{uy3}$) | kN · s/m | 23.21 |
| Upper vertical damper damping coefficient ($C_{uz2}=C_{uz4}$) | kN · s/m | 5.18 |
| Upper lateral damper damping coefficient ($C_{uy2}=C_{uy4}$) | kN · s/m | 5.18 |
| Lower vertical spring stiffness ($K_{lz1}=K_{lz2}=K_{lz3}=K_{lz4}$) | kN/m | 351 |
| Lower lateral spring stiffness ($K_{ly1}=K_{ly2}=K_{ly3}=K_{ly4}$) | kN/m | 121 |
| Lower vertical damper damping coefficient ($C_{lz1}=C_{lz2}=C_{lz3}=C_{lz4}$) | kN · s/m | 0.80 |
| Lower lateral damper damping coefficient ($C_{ly1}=C_{ly2}=C_{ly3}=C_{ly4}$) | kN · s/m | 0.80 |
| Reference area (A_f) | m ² | 10.50 |
| Reference height (h_v) | m | 1.50 |
| Distance (L_1) | m | 3.00 |
| Distance (L_2) | m | 5.00 |
| Distance (b_1) | m | 1.10 |
| Distance (h_1) | m | 0.80 |

$$\begin{aligned}
M_v \ddot{Z}_v + C_{uz1}(\dot{Z}_v - L_1 \dot{\theta}_v - b_1 \dot{\phi}_v - \dot{Z}_{s1}) + C_{uz2}(\dot{Z}_v + L_2 \dot{\theta}_v - b_1 \dot{\phi}_v - \dot{Z}_{s2}) + C_{uz3}(\dot{Z}_v - L_1 \dot{\theta}_v + b_1 \dot{\phi}_v - \dot{Z}_{s3}) \\
+ C_{uz4}(\dot{Z}_v + L_2 \dot{\theta}_v + b_1 \dot{\phi}_v - \dot{Z}_{s4}) + K_{uz1}(Z_v - L_1 \theta_v - b_1 \phi_v - Z_{s1}) + K_{uz2}(Z_v + L_2 \theta_v - b_1 \phi_v - Z_{s2}) \\
+ K_{uz3}(Z_v - L_1 \theta_v + b_1 \phi_v - Z_{s3}) + K_{uz4}(Z_v + L_2 \theta_v + b_1 \phi_v - Z_{s4}) = F_{vzw}
\end{aligned} \quad (15)$$

where F_{vzw} is the aerodynamic force acting on the vehicle body in the Z-direction.

The dynamic equilibrium condition of the vehicle body about the X-axis leads to

$$\begin{aligned}
J_{xv} \ddot{\phi}_v - C_{uz1}(\dot{Z}_v - L_1 \dot{\theta}_v - b_1 \dot{\phi}_v - \dot{Z}_{s1}) b_1 - C_{uz2}(\dot{Z}_v + L_2 \dot{\theta}_v - b_1 \dot{\phi}_v - \dot{Z}_{s2}) b_1 + C_{uz3}(\dot{Z}_v - L_1 \dot{\theta}_v + b_1 \dot{\phi}_v - \dot{Z}_{s3}) b_1 \\
+ C_{uz4}(\dot{Z}_v + L_2 \dot{\theta}_v + b_1 \dot{\phi}_v - \dot{Z}_{s4}) b_1 - K_{uz1}(Z_v - L_1 \theta_v - b_1 \phi_v - Z_{s1}) b_1 - K_{uz2}(Z_v + L_2 \theta_v - b_1 \phi_v - Z_{s2}) b_1 \\
+ K_{uz3}(Z_v - L_1 \theta_v + b_1 \phi_v - Z_{s3}) b_1 + K_{uz4}(Z_v + L_2 \theta_v + b_1 \phi_v - Z_{s4}) b_1 \\
+ C_{uy1}(\dot{Y}_v + h_1 \dot{\phi}_v + L_1 \dot{\phi}_v - \dot{Y}_{s1}) h_1 + C_{uy2}(\dot{Y}_v + h_1 \dot{\phi}_v - L_2 \dot{\phi}_v - \dot{Y}_{s2}) h_1 + C_{uy3}(\dot{Y}_v + h_1 \dot{\phi}_v + L_1 \dot{\phi}_v - \dot{Y}_{s3}) h_1 \\
+ C_{uy4}(\dot{Y}_v + h_1 \dot{\phi}_v - L_2 \dot{\phi}_v - \dot{Y}_{s4}) h_1 + K_{uy1}(Y_v + h_1 \phi_v + L_1 \phi_v - Y_{s1}) h_1 + K_{uy2}(Y_v + h_1 \phi_v - L_2 \phi_v - Y_{s2}) h_1 \\
+ K_{uy3}(Y_v + h_1 \phi_v + L_1 \phi_v - Y_{s3}) h_1 + K_{uy4}(Y_v + h_1 \phi_v - L_2 \phi_v - Y_{s4}) h_1 = M_{vxx}
\end{aligned} \quad (16)$$

where M_{vxw} is the aerodynamic moment acting on the vehicle body about the X-axis.

The dynamic equilibrium condition of the vehicle body about the Y-axis yields

$$\begin{aligned} J_{yv} \ddot{\theta}_v - C_{uz1}(\dot{Z}_v - L_1 \dot{\theta}_v - b_1 \dot{\phi}_v - \dot{Z}_{s1})L_1 + C_{uz2}(\dot{Z}_v + L_2 \dot{\theta}_v - b_1 \dot{\phi}_v - \dot{Z}_{s2})L_2 - C_{uz3}(\dot{Z}_v - L_1 \dot{\theta}_v + b_1 \dot{\phi}_v - \dot{Z}_{s3})L_1 \\ + C_{uz4}(\dot{Z}_v + L_2 \dot{\theta}_v + b_1 \dot{\phi}_v - \dot{Z}_{s4})L_2 - K_{uz1}(Z_v - L_1 \theta_v - b_1 \phi_v - Z_{s1})L_1 + K_{uz2}(Z_v + L_2 \theta_v - b_1 \phi_v - Z_{s2})L_2 \\ - K_{uz3}(Z_v - L_1 \theta_v + b_1 \phi_v - Z_{s3})L_1 + K_{uz4}(Z_v + L_2 \theta_v + b_1 \phi_v - Z_{s4})L_2 = M_{vyw} \end{aligned} \quad (17)$$

where M_{vyw} is the aerodynamic moment acting on the vehicle body about the Y-axis.

The dynamic equilibrium condition of the vehicle body about the Z-axis results in

$$\begin{aligned} J_{zv} \ddot{\phi}_v + C_{uy1}(\dot{Y}_v + h_1 \dot{\phi}_v + L_1 \dot{\phi}_v - \dot{Y}_{s1})L_1 - C_{uy2}(\dot{Y}_v + h_1 \dot{\phi}_v - L_2 \dot{\phi}_v - \dot{Y}_{s2})L_2 + C_{uy3}(\dot{Y}_v + h_1 \dot{\phi}_v + L_1 \dot{\phi}_v - \dot{Y}_{s3})L_1 \\ - C_{uy4}(\dot{Y}_v + h_1 \dot{\phi}_v - L_2 \dot{\phi}_v - \dot{Y}_{s4})L_2 + K_{uy1}(Y_v + h_1 \phi_v + L_1 \phi_v - Y_{s1})L_1 - K_{uy2}(Y_v + h_1 \phi_v - L_2 \phi_v - Y_{s2})L_2 \\ + K_{uy3}(Y_v + h_1 \phi_v + L_1 \phi_v - Y_{s3})L_1 - K_{uy4}(Y_v + h_1 \phi_v - L_2 \phi_v - Y_{s4})L_2 = M_{vzw} \end{aligned} \quad (18)$$

where M_{vzw} is the aerodynamic moment acting on the vehicle body about the Z-axis.

The equations of motion of the left rigid body in the front axle set in the Y- and Z-directions can be expressed as

$$\begin{aligned} M_{s1} \ddot{Y}_{s1} - C_{uy1}(\dot{Y}_v + h_1 \dot{\phi}_v + L_1 \dot{\phi}_v - \dot{Y}_{s1}) - K_{uy1}(Y_v + h_1 \phi_v + L_1 \phi_v - Y_{s1}) \\ + C_{ly1}(\dot{Y}_{s1} - \dot{Y}_{c1}) + K_{ly1}(Y_{s1} - Y_{c1}) = 0 \end{aligned} \quad (19)$$

$$\begin{aligned} M_{s1} \ddot{Z}_{s1} - C_{uz1}(\dot{Z}_v - L_1 \dot{\theta}_v - b_1 \dot{\phi}_v - \dot{Z}_{s1}) - K_{uz1}(Z_v - L_1 \theta_v - b_1 \phi_v - Z_{s1}) \\ + C_{lz1}(\dot{Z}_{s1} - \dot{Z}_{c1}) + K_{lz1}(Z_{s1} - Z_{c1}) = 0 \end{aligned} \quad (20)$$

The equations of motion of the left rigid body in the rear axle set in the Y- and Z-directions can be expressed as

$$\begin{aligned} M_{s2} \ddot{Y}_{s2} - C_{uy2}(\dot{Y}_v + h_1 \dot{\phi}_v - L_2 \dot{\phi}_v - \dot{Y}_{s2}) - K_{uy2}(Y_v + h_1 \phi_v - L_2 \phi_v - Y_{s2}) \\ + C_{ly2}(\dot{Y}_{s2} - \dot{Y}_{c2}) + K_{ly2}(Y_{s2} - Y_{c2}) = 0 \end{aligned} \quad (21)$$

$$\begin{aligned} M_{s2} \ddot{Z}_{s2} - C_{uz2}(\dot{Z}_v + L_2 \dot{\theta}_v - b_1 \dot{\phi}_v - \dot{Z}_{s2}) - K_{uz2}(Z_v + L_2 \theta_v - b_1 \phi_v - Z_{s2}) \\ + C_{lz2}(\dot{Z}_{s2} - \dot{Z}_{c2}) + K_{lz2}(Z_{s2} - Z_{c2}) = 0 \end{aligned} \quad (22)$$

The equations of motion of the right rigid body in the front axle set in the Y- and Z-directions can be written as

$$\begin{aligned} M_{s3} \ddot{Y}_{s3} - C_{uy3}(\dot{Y}_v + h_1 \dot{\phi}_v + L_1 \dot{\phi}_v - \dot{Y}_{s3}) - K_{uy3}(Y_v + h_1 \phi_v + L_1 \phi_v - Y_{s3}) \\ + C_{ly3}(\dot{Y}_{s3} - \dot{Y}_{c3}) + K_{ly3}(Y_{s3} - Y_{c3}) = 0 \end{aligned} \quad (23)$$

$$\begin{aligned} M_{s3} \ddot{Z}_{s3} - C_{uz3}(\dot{Z}_v - L_1 \dot{\theta}_v + b_1 \dot{\phi}_v - \dot{Z}_{s3}) - K_{uz3}(Z_v - L_1 \theta_v + b_1 \phi_v - Z_{s3}) \\ + C_{lz3}(\dot{Z}_{s3} - \dot{Z}_{c3}) + K_{lz3}(Z_{s3} - Z_{c3}) = 0 \end{aligned} \quad (24)$$

The equations of motion of the right rigid body in the rear axle set in the Y - and Z -directions can be written as

$$\begin{aligned} M_{s4}\ddot{Y}_{s4} - C_{uy4}(\dot{Y}_v + h_1\dot{\phi}_v - L_2\dot{\phi}_v - \dot{Y}_{s4}) - K_{uy4}(Y_v + h_1\phi_v - L_2\phi_v - Y_{s4}) \\ + C_{ly4}(\dot{Y}_{s4} - \dot{Y}_{c4}) + K_{ly4}(Y_{s4} - Y_{c4}) = 0 \end{aligned} \quad (25)$$

$$\begin{aligned} M_{s4}\ddot{Z}_{s4} - C_{uz4}(\dot{Z}_v + L_2\dot{\theta}_v + b_1\dot{\phi}_v - \dot{Z}_{s4}) - K_{uz4}(Z_v + L_2\theta_v + b_1\phi_v - Z_{s4}) \\ + C_{lz4}(\dot{Z}_{s4} - \dot{Z}_{c4}) + K_{lz4}(Z_{s4} - Z_{c4}) = 0 \end{aligned} \quad (26)$$

In Eqs. (20), (22), (24), and (26), Z_{ci} ($i=1, 2, \dots, 4$) denotes the vertical displacement of the i th tyre. With the assumption that the vertical road surface profile is not too rough to make the vehicle jump or leave the riding surface, the tyre of the vehicle is assumed to be a point and remains in contact with the road surface at all times except for the occurrence of overturning accident. As a result, the vertical displacement, velocity and acceleration of each contact point can be expressed in terms of the road surface profile.

$$Z_{ci} = r_{ci}(x) \quad (27)$$

$$\dot{Z}_{ci} = \frac{\partial r_{ci}(x)}{\partial x} U_v \quad (28)$$

$$\ddot{Z}_{ci} = \frac{\partial^2 r_{ci}(x)}{\partial x^2} U_v^2 \quad (29)$$

where $r_{ci}(x)$ is the road surface roughness under the i th contact point. Clearly, Z_{ci} ($i=1, 2, \dots, 4$) and its derivatives are known quantities so that they do not appear as independent degrees of freedom.

The consideration of dynamic equilibrium condition of each tyre in the Y -direction yields

$$M_{ci}\ddot{Y}_{ci} + C_{lyi}(\dot{Y}_{ci} - \dot{Y}_{si}) + K_{lyi}(Y_{ci} - Y_{si}) = F_{hi} \quad (i=1, 2, \dots, 4) \quad (30)$$

where F_{hi} ($i=1, 2, \dots, 4$) is the lateral contact force between the i th tyre and the road surface, namely the tyre sideslip force.

The tyre sideslip forces can be related, very approximately, to the vertical reactions by equations of the form (Baker 1986).

$$F_{hi} = -m \left(\frac{\dot{Y}_{ci}}{U_v} + \delta \right) F_{vi} \quad (i=1, 3) \quad (31)$$

$$F_{hi} = -m \frac{\dot{Y}_{ci}}{U_v} F_{vi} \quad (i=2, 4) \quad (32)$$

where m is a coefficient of sideslip friction, and the negative sign ensures that the sideslip force resists the lateral motion of the tyre relative to the road surface; F_{vi} is the vertical contact force between the i th tyre and the road surface; and δ is a steering angle, that is the angle of the front

wheels to the vehicle axis. The introduction of the steering angle of the front wheels is to consider driver behaviour for course correction, but it is not necessary in this study as mentioned before. It is noted that Eqs. (31) and (32) control the sideslip of the vehicle and introduce the nonlinear terms to the governing equations of motion of the vehicle. Substituting Eqs. (31) and (32) into Eq. (30) then yields

$$M_{ci}\ddot{Y}_{ci} + \left(C_{lyi} + m \frac{F_{vi}}{U_v} \right) \dot{Y}_{ci} - C_{lyi} \dot{Y}_{si} + K_{lyi}(Y_{ci} - Y_{si}) = -\delta m F_{vi} \quad (i=1, 3) \quad (33)$$

$$M_{ci}\ddot{Y}_{ci} + \left(C_{lyi} + m \frac{F_{vi}}{U_v} \right) \dot{Y}_{ci} - C_{lyi} \dot{Y}_{si} + K_{lyi}(Y_{ci} - Y_{si}) = 0 \quad (i=2, 4) \quad (34)$$

The vertical contact forces are given by

$$F_{vi} = M_{ci}\ddot{Z}_{ci} + C_{lzi}(\dot{Z}_{ci} - \dot{Z}_{si}) + K_{lzi}(Z_{ci} - Z_{si}) + F_{Gi} \quad (i=1, 2, \dots, 4) \quad (35)$$

where F_{Gi} ($i=1, 2, \dots, 4$) is the force on the i th tyre due to the gravity of the vehicle, which can be calculated by

$$F_{Gi} = M_v g \frac{L_2}{2(L_1 + L_2)} + (M_{si} + M_{ci})g \quad (i=1, 3) \quad (36)$$

$$F_{Gi} = M_v g \frac{L_1}{2(L_1 + L_2)} + (M_{si} + M_{ci})g \quad (i=2, 4) \quad (37)$$

where g is the acceleration due to gravity.

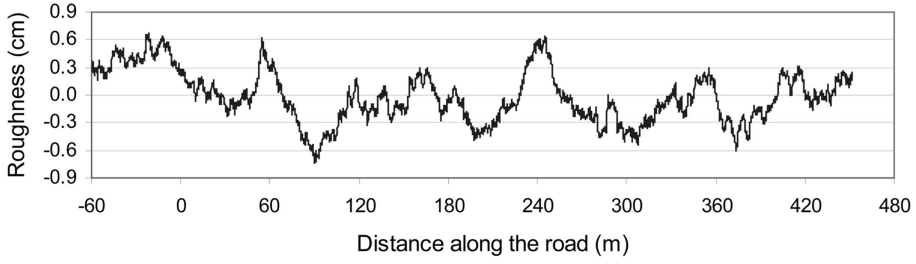
Eqs. (14) to (26) and Eqs. (33) and (34) are regarded as the governing equations of motion of a high-sided road vehicle running on the road at a constant velocity and subjected to a sudden crosswind gust. However, Eqs. (33) and (34) are nonlinear equations because the time varying vertical contact forces expressed by Eq. (35) are functions of the motions of the front axle set and the rear axle set in the Z -direction (Z_{si}) which are coupled with the motions of the front axle set and the rear axle set in the Y -direction (Y_{si}). Thus, iterations have to be used at each time step in order to find the numerical solution of the governing equations of motion of the vehicle.

The two rigid bodies in either the front axle set or the rear axle set are connected by a massless rigid rod in this numerical study. The following two restriction equations are used to reduce the number of governing equations of motion from 17 to 15.

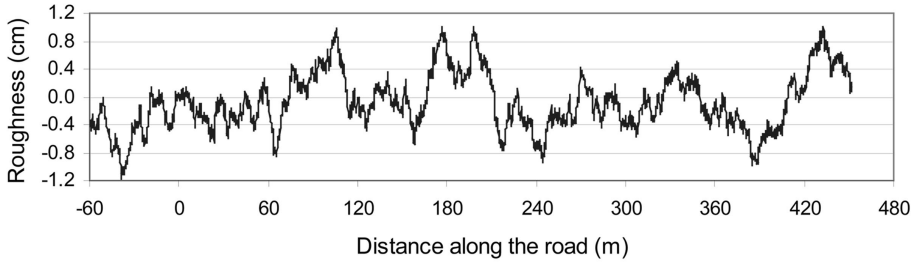
$$Y_{s1} = Y_{s3} \quad (38)$$

$$Y_{s2} = Y_{s4} \quad (39)$$

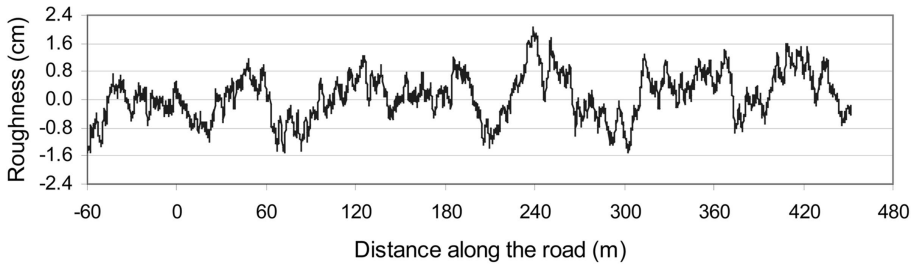
The selected vehicle in this study is similar to that investigated by Coleman and Baker (1990) for ground vehicles under cross winds. The following formulae were suggested for determining the aerodynamic force and moment coefficients of the vehicle as a function of the yaw angle.



(a) Very good road condition



(b) Good road condition



(c) Average road condition

Fig. 3 Vertical road surface profiles

$$C_s(\psi) = 5.2(\psi)^{0.382} \quad (40)$$

$$C_L(\psi) = 0.93(1 + \sin 3\psi) \quad (41)$$

$$C_D(\psi) = 0.5(1 + 2\sin 3\psi) \quad (42)$$

$$C_Y(\psi) = -2.0(\psi)^{1.77} \quad (43)$$

$$C_P(\psi) = -2.0(\psi)^{1.32} \quad (44)$$

$$C_R(\psi) = 7.3(\Psi)^{0.294} \quad (45)$$

These force and moment coefficients were obtained with respect to the gravity centre of the vehicle body. The value of roughness coefficient A_r in Eq. (3) is taken as 80×10^{-6} , 20×10^{-6} and 5×10^{-6} m³/cycle for the average, good, and very good road surface, respectively. A total of 16384 (2^{14}) data points are generated within the sample length of 2048 m. Such long sample lengths may not be

necessary for this study, but they will be used in other relevant studies. The vertical road surface profile averaged from 5 simulations with the first 512 m is shown in Fig. 3(a), 3(b), and 3(c), respectively, for very good, good, and average road conditions.

6. Numerical results

6.1. Solution of equations of motion

A computer program for determining the dynamic response and the accident vehicle speed of a moving road vehicle subject to a sudden crosswind gust was developed according to the proposed framework. The equations of motion assembled by the computer program were a set of coupled second order nonlinear differential equations. The Wilson- θ method was used in this study to find the solutions (Chopra 1995). The θ value and the time interval used in the computation were 1.4 and 0.005 second, respectively. Within each time step, the iterations were performed in consideration of the sideslip forces between the tyre and the road surface.

To properly simulate the case in which a moving road vehicle was subjected to a sudden crosswind gust, the x -axis was set along the road with the coordinate of -60 m for the starting point of the road surface profile, as shown in Fig. 4. The x -coordinate of the initial position of the centroid of the vehicle body was taken as -50 m, where the vehicle started to run with all the initial conditions being zero except for the vehicle speed in the x -direction. When the vehicle run to the place with the zero x -coordinate for its centroid, a sudden crosswind gust was imposed on the vehicle. When the centroid of the vehicle body was of negative x -coordinate, there was no crosswind and the relative wind velocity became the same as the vehicle velocity in the x -direction. Since the corresponding wind lift force due to the relative wind velocity (i.e., the vehicle velocity) was very small, it was neglected and the vibration source of the vehicle was only the road surface roughness. As the centroid of the vehicle body moved to the location of positive x -coordinate, the vibration sources of the vehicle included both the road surface roughness and the sudden crosswind gust. The total computation time required was thus the sum of the time during which the vehicle run through the first 50 m long road without wind forces and 0.5 second during which the vehicle entered into a sharp-edged crosswind gust.

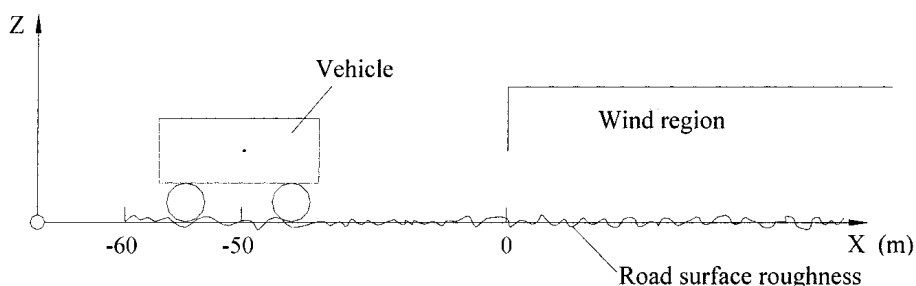
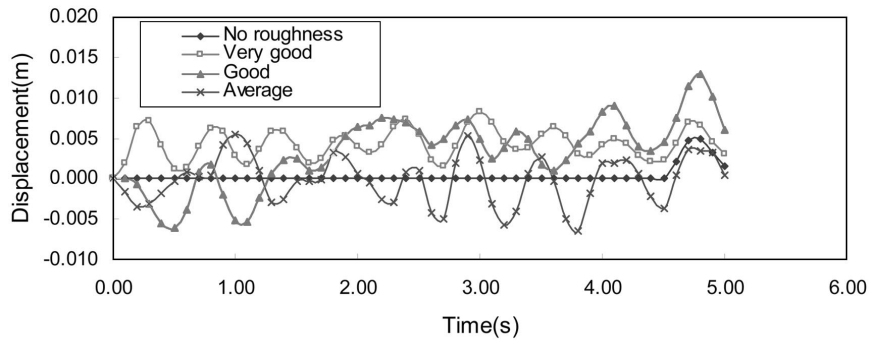


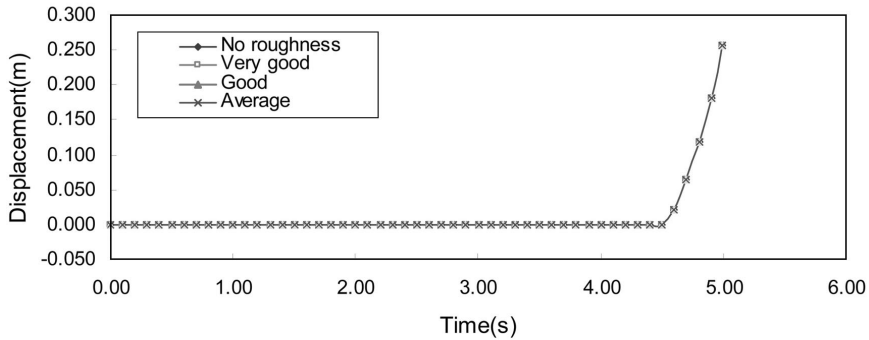
Fig. 4 The x -coordinates used for a moving road vehicle

6.2. Effects of road surface roughness

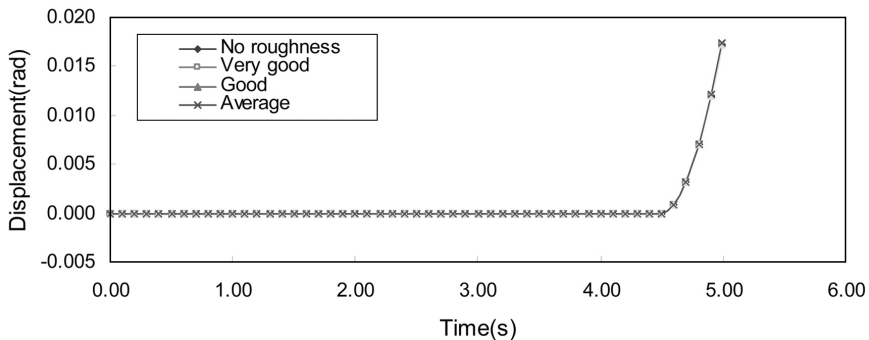
Displayed in Fig. 5(a) are the time histories of the vertical displacement responses (Z_v) of the vehicle at its centroid for four road surface conditions in the vertical direction: no roughness, very good, good, and average road conditions. The value of roughness coefficient A_r in Eq. (3) is taken as 5×10^{-6} , 20×10^{-6} , $80 \times 10^{-6} \text{ m}^3/\text{cycle}$ for the very good, good and average road surface, respectively, according to Wang and Huang (1992), which is consistent with the value specified by



(a) Vertical Displacement



(b) Lateral Displacement



(c) Rotational Displacement

Fig. 5 Effects of road roughness on dynamic displacement responses ($U_v=40 \text{ km/h}$, $U_m=20 \text{ m/s}$)

the International Organization for Standardization (ISO). The vehicle speed used in the computation is constant of 40 km/h, and the sudden crosswind gust is of 20 m/s. It thus takes 4.5 seconds for the vehicle to run through a 50 m distance without wind forces and then to enter a sudden crosswind gust for 0.5 second. It is seen from Fig. 5(a) that within the first 4.5 seconds, the vertical displacement response remains zero for the vehicle running on the road of no roughness. When the vehicle runs on the road of roughness, the vehicle vibrates vertically with a dominant frequency around the first natural frequency of the vehicle in the vertical direction. The vertical displacement response of the vehicle depends on the road surface profile as shown in Fig. 3. When the vehicle enters a sudden crosswind gust at 4.5 second, the vehicle experiences a vertical vibration even when it runs on the road of no roughness. The peak response of the vehicle, however, depends on the road surface and the initial condition of the vehicle when it enters the sudden crosswind gust.

The time histories of the lateral and rotational displacement responses of the vehicle are plotted in Fig. 5(b) and Fig. 5(c), respectively. During the first 4.5 seconds when there is no wind force acting on the vehicle, the lateral and rotational displacement responses of the vehicle remain zero. Afterwards, the lateral and rotational displacement responses of the vehicle increase rapidly due to suddenly applied wind forces. For instance, the lateral displacement response of the vehicle at its centroid, Y_v , is zero at 4.5 second but it reaches 0.256 m at 5.0 second. Such a lateral displacement response is actually the algebraic summation of two parts: one is the motion of the vehicle as a whole due to the sideslip; and the other is the vibration of the vehicle itself. For this case, the sideslip of the vehicle at the front left tyre, Y_{c1} , is computed as 0.246 m. The total lateral displacement of the front axle set, Y_{s1} , is 0.274 m. As a result, the relative lateral displacement of the vehicle at its centroid to its front axle set is 0.018 m only and the relative lateral displacement of the front axle set to the front left tyre is 0.028 m only. These results show that even though the total lateral displacement of the vehicle at its centroid is quite large but its relative displacement within the vehicle is quite small to comply with the small displacement assumption. It is also seen that both the lateral and rotational displacement responses of the vehicle keep the same for all the road conditions concerned. This indicates that the vertical road surface condition does not affect the lateral and rotational displacement responses of the vehicle.

Figs. 6(a) to 6(d) show the time histories of vertical contact forces acting on the 1st, 2nd, 3rd, and 4th tyres, respectively. During the first 4.5 seconds when the vehicle runs on the road of no roughness and without wind forces, the vertical contact forces acting on the 1st, 2nd, 3rd, and 4th tyres remain constant of 21.58, 15.21, 21.58, and 15.21 kN, respectively. These constant contact forces on the tyres are solely determined by the gravity force of the vehicle, for there are no wind forces and no road roughness. Furthermore, because of the symmetry of the vehicle with respect to the x -axis, the contact force on the 1st tyre is the same as that on the 3rd tyre while the contact force on the 2nd tyre is the same as that on the 4th tyre. When the vehicle runs on the road of roughness, the contact forces fluctuate around the constant contact forces caused by the gravity force of the vehicle. It is clear that within the first 4.5 seconds, the better is the road condition, the smaller is the peak contact force for any one of the four tyres. When the vehicle enters into a sudden crosswind gust, the contact forces on the 1st and 2nd tyres that are on the windward side significantly decreases whereas the contact forces on 3rd and 4th tyre that are on the leeward side considerably increase, compared with the constant contact forces in the first 4.5 seconds. The decrease of peak contact forces on the windward tyres and the increase of peak contact forces on the leeward tyres are larger for rougher road condition. The minimum peak contact force occurs on the 2nd tyre of 2.52, 4.50, 5.12, and 5.22 kN for the average, good, very good, and no roughness

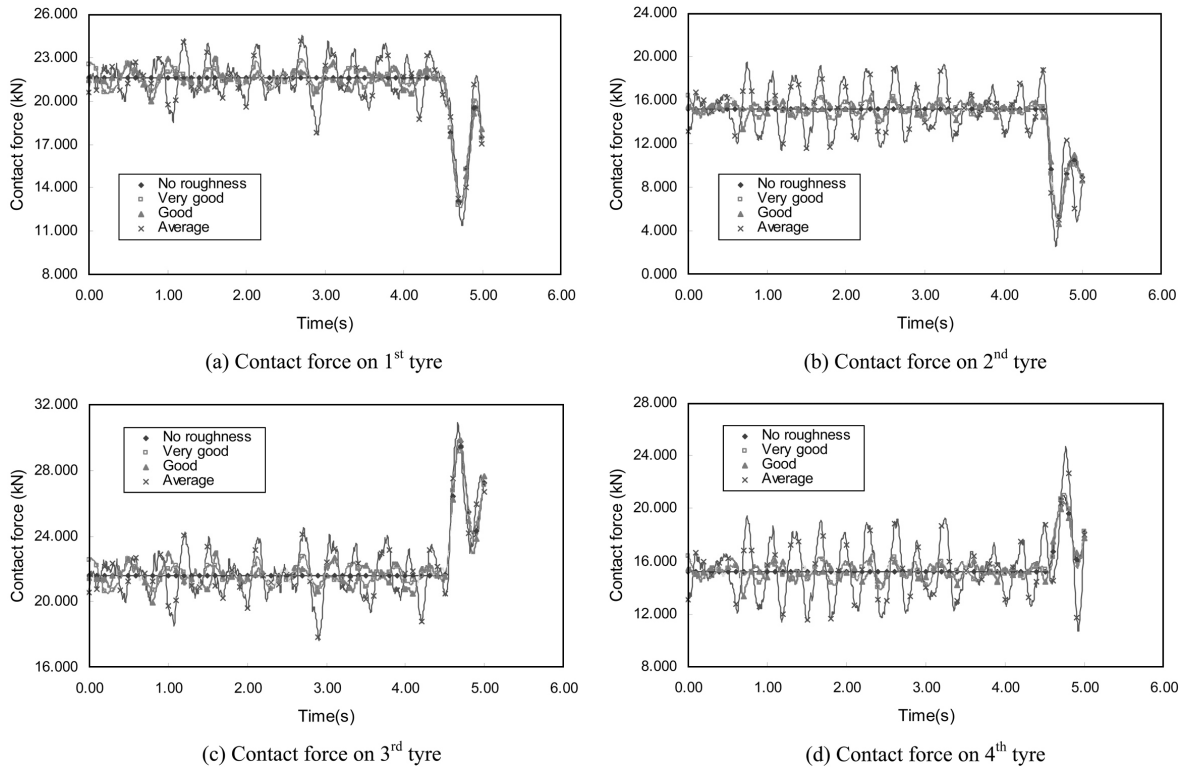
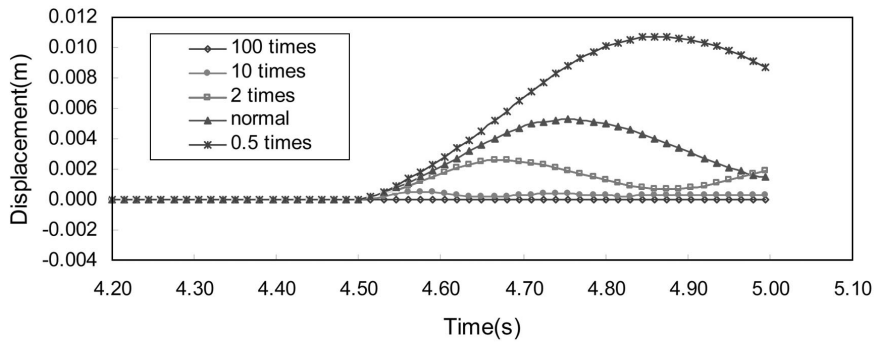


Fig. 6 Effects of road roughness on contact forces ($U_v=40$ km/h, $U_m=20$ m/s)

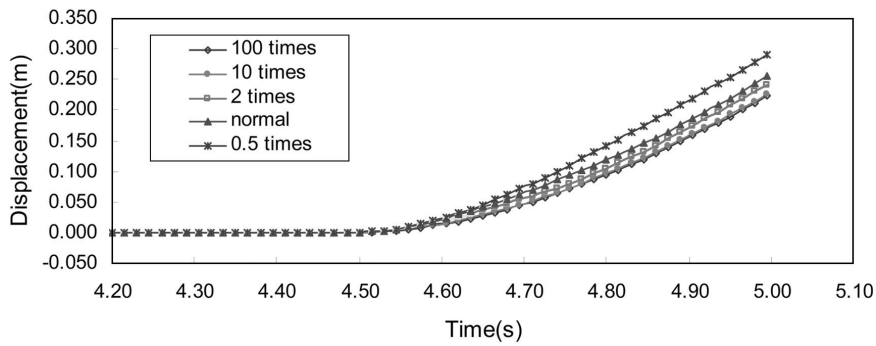
road conditions, respectively. These results indicate that the overturning accident of the vehicle is controlled by the 2nd tyre. The rougher is the road condition, the smaller is the contact force on the 2nd tyre. From the above discussions, one may conclude that the road surface condition in the vertical direction does affect the vertical displacement response of the vehicle and the contact forces on the vehicle tyres. They may in turn affect the accident vehicle speed for a given gust wind speed.

6.3. Effects of vehicle suspension system

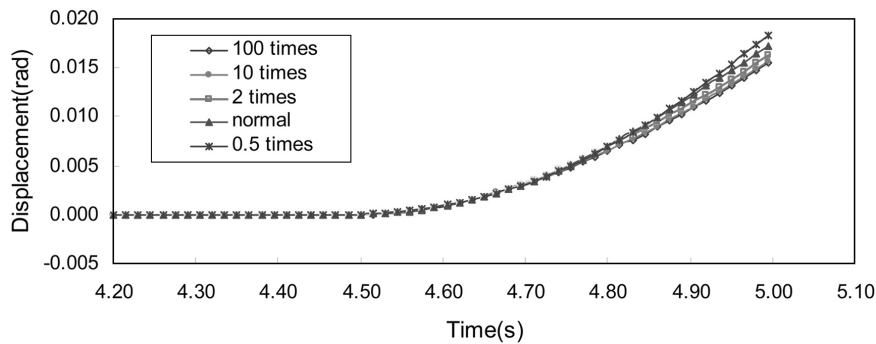
To investigate the effects of vehicle suspension system on the dynamic performance of the vehicle, all the spring stiffness coefficients and damper damping coefficients of the vehicle, as listed in Table 1, are multiplied by the same value of 100, 10, 2, 1 (normal), and 0.5, respectively, to form the suspension systems of No. 1, 2, 3, 4, and 5 correspondingly. The multiplication factor over 10 is not realistic but it implies the rigid suspension assumption used in the previous study (Baker 1986) so that the validity of this assumption can be assessed. Other parameters of the vehicle, such as the geometric dimension, the mass, and the mass moments of inertia, remain unchanged. As a result, the first natural frequency of the vehicle is 9.80, 3.10, 1.39, 0.98, and 0.69 Hz in the lateral direction, and 18.60, 5.71, 2.55, 1.81, and 1.28 Hz in the vertical direction, corresponding to the suspension systems of No.1, 2, 3, 4, and 5, respectively. The discussion in the last section is for the No. 4 suspension system (normal system). To have a reasonable comparison between different



(a) Vertical Displacement



(b) Lateral Displacement



(c) Rotational Displacement

Fig. 7 Effects of vehicle suspension on dynamic displacement responses ($U_v=40$ km/h, $U_m=20$ m/s)

vehicle suspension systems, the dynamic analyses of the vehicle are carried out for the vehicle running on the road of no roughness and the results obtained are presented in the following.

Fig. 7(a) shows the time histories of vertical displacement responses of the vehicle for different suspension systems at a vehicle speed of 40 km/h and under a sudden crosswind gust of 20 m/s. It is seen that during the first 4.5 seconds when the vehicle runs on the smooth road without wind forces, the vertical displacement response of the vehicle remains zero for all types of suspension systems. When the vehicle enters into a sudden crosswind gust, it experiences vertical vibration.

The peak vertical displacement response of the vehicle increases from zero to 0.0, 0.5, 2.6, 5.3, and 10.7 mm, respectively, corresponding to the suspension systems of No. 1, 2, 3, 4, and 5. Clearly, the softer is the spring stiffness and the lighter is the damper damping, the larger is the peak displacement response of the vehicle when it is subjected to a sudden crosswind gust.

Depicted in Figs. 7(b) and 7(c) are the time histories of lateral and rotational displacements of the vehicle for different suspension systems at a vehicle speed of 40 km/h and under a sudden crosswind gust of 20 m/s. Again, during the first 4.5 seconds when the vehicle runs on the road without wind forces, all the lateral and rotational displacement responses of the vehicle remain zero because there are no any wind forces and road roughness affecting the vehicle. When the vehicle enters a sudden crosswind gust, the lateral and rotational displacement responses of the vehicle increase monotonously with time. At a given time, the lateral and rotational displacement responses increase with the increase in the number of the suspension system. The maximum lateral displacement responses of the vehicle occur at 5.0 seconds. They are 0.22, 0.23, 0.24, 0.26, and 0.29 m for the suspension systems of No. 1, 2, 3, 4, and 5, respectively. The maximum rotational displacement responses of the vehicle also occur at 5.0 seconds. They are 0.0155, 0.0156, 0.0163, 0.0172, and 0.0184 radian for the suspension systems of No. 1, 2, 3, 4, and 5, respectively. Clearly, the softer is the spring stiffness and the lighter is the damper damping, the larger is the lateral and rotational displacement responses.

Plotted in Figs. 8(a) to (d) are the time histories of vertical contact forces on the 1st, 2nd, 3rd, and

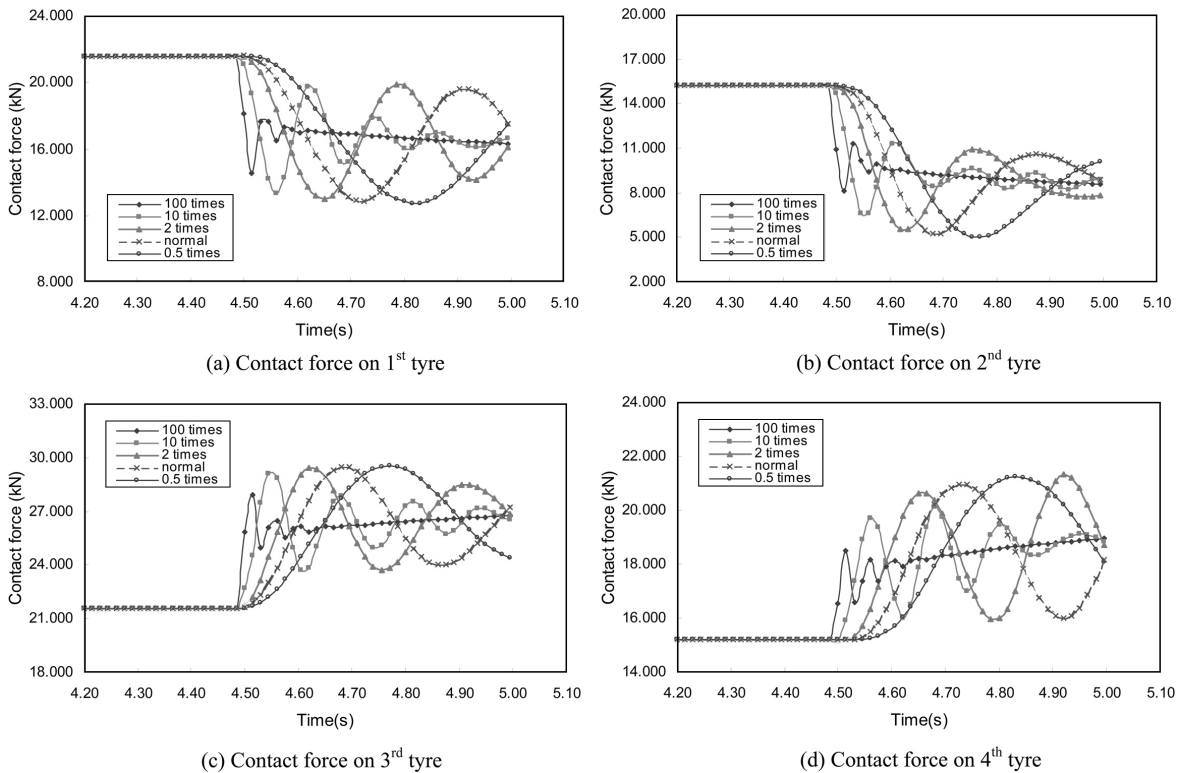


Fig. 8 Effects of vehicle suspension on contact forces ($U_v=40$ km/h, $U_m=20$ m/s)

4th tyres, respectively. During the first 4.5 seconds when the vehicle runs on the road of no roughness and without wind forces, the vertical contact forces on the 1st and 3rd tyres remain unchanged at 21.58 kN whereas the contact forces on the 2nd and 4th tyres remain at 15.21 kN. These vertical contact forces are caused by the vehicle weight only. When the vehicle enters a sudden crosswind gust, the vertical contact forces on the windward 1st and 2nd tyres have a sudden decrease whereas those on the leeward 3rd and 4th tyres have a sudden increase. Afterwards, the contact force on each tyre fluctuates at the natural frequency of the vehicle and around a new dynamic equilibrium position. The contact forces on each tyre for different suspension systems finally reach a common value, which is determined by both the static wind forces and the weight of the vehicle. Again, the minimum contact force occurs on the 2nd tyre of 7.94, 6.36, 5.49, 5.22, and 5.02 kN for the suspension systems of No. 1, 2, 3, 4, and 5, respectively. Therefore, one may conclude that the vehicle suspension does affect the dynamic responses and contact forces of the vehicle subject to a sudden crosswind gust. The suspension systems of softer spring and lighter damper may lead to a lower accident vehicle speed for a given wind speed.

6.4. Accident vehicle speed

To investigate the effects of road surface roughness on the accident vehicle speed of the high-sided road vehicle selected, the suspension system of the vehicle is taken as the normal case (No. 4) and the four road conditions are considered: no roughness, very good, good, and average road surfaces. The computation is carried out in such a way that for a given road condition and a given sudden crosswind speed, the dynamic responses and contact forces of the moving vehicle are computed at a series of vehicle speed in an ascending order. The increment of the vehicle speed is taken as 2.5 km/h. If the dynamic responses and contact forces computed indicate that wind-induced vehicle accident does not occur, a higher vehicle speed that equals the current vehicle speed plus the vehicle speed increment of 2.5 km/h will be adopted for the next step computation until the computation results showing that at least one type of vehicle accident occurs. Correspondingly, the final vehicle speed is called the accident vehicle speed for the wind speed specified.

The computed accident vehicle speeds for different road surface conditions are plotted in Fig. 9 and listed in Table 2 together with the type of vehicle accidents. It is seen that with the increase in gust wind speed, the accident vehicle speed decreases. For a given crosswind speed, a better road

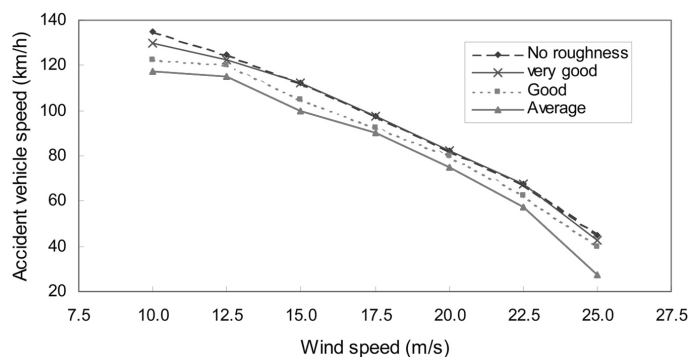


Fig. 9 Effects of road roughness on accident vehicle speed

Table 2 Accident vehicle speeds for different road conditions (normal suspension system No.4)

| Mean wind speed (m/s) | Average (km/h) | Good (km/h) | Very good (km/h) | No roughness (km/h) |
|-----------------------|----------------|-------------|------------------|---------------------|
| 10.0 | 117.5 (o) | 122.5 (o) | 130.0 (o) | 135.0 (s) |
| 12.5 | 115.0 (o) | 120.0 (o) | 122.5 (o) | 125.0 (o) |
| 15.0 | 100.0 (o) | 105.0 (o) | 112.5 (o) | 112.5 (o) |
| 17.5 | 90.0 (o) | 92.5 (o) | 97.5 (o) | 97.5 (o) |
| 20.0 | 75.0 (o) | 80.0 (o) | 82.5 (o) | 82.5 (o) |
| 22.5 | 57.5 (o) | 62.5 (o) | 67.5 (o) | 67.5 (o) |
| 25.0 | 27.5 (o) | 40.0 (o) | 42.5 (o) | 45.0 (o) |

Note: o-Overturning accident; s-Sideslip accident; r-Rotation accident.

condition leads to a relatively higher accident vehicle speed. For a given vehicle speed, a better road condition gives a relatively higher accident wind speed. The safety of the concerned high-sided road vehicle subject to a sudden crosswind gust is mainly controlled by overturning accident, except that only one case, in which the crosswind speed is 10 m/s and the road has no roughness, is controlled by sideslip accident with the accident vehicle speed of 135 km/h.

To investigate the effects of vehicle suspension on the accident vehicle speed of the high-sided road vehicle selected, the suspension systems of the vehicle from No. 1 to No. 5 are considered but only one road condition, that is, no roughness is selected for the computation. The computation is carried out in such a way that for a given suspension system and a given sudden crosswind speed, the dynamic responses and contact forces of the moving vehicle are computed at a series of vehicle speed in an ascending order of an increment of 2.5 km/h until the computation results showing that at least one type of vehicle accident occurs. The obtained accident vehicle speed for different suspension systems are plotted in Fig. 10 and listed in Table 3. It is seen that with the increase in the gust wind speed, the accident vehicle speed decreases. For a given crosswind speed, the softer suspension system leads to a lower accident vehicle speed. For a given vehicle speed, the softer suspension system results in a lower accident wind speed. It is interesting to see that for the suspension system of the highest spring stiffness and the heaviest damper damping (No. 1), all the vehicle accidents are the sideslip accident (see Table 3). For the suspension system of smaller spring

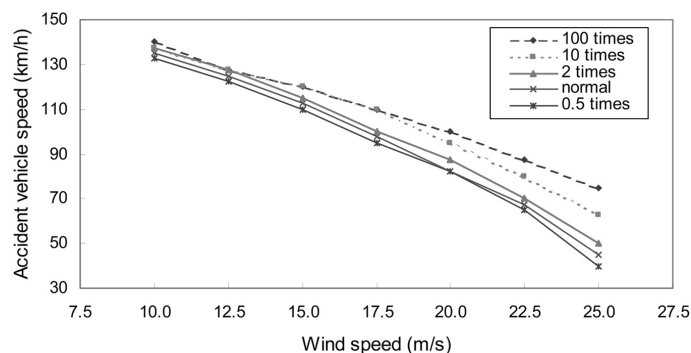


Fig. 10 Effects of vehicle suspension on accident vehicle speed

Table 3 Accident vehicle speeds for different suspension systems (no roughness)

| Mean wind speed (m/s) | 100 times (km/h) | 10 times (km/h) | 2 times (km/h) | Normal (km/h) | 0.5 times (km/h) |
|--------------------------|---------------------|--------------------|-------------------|------------------|---------------------|
| 10.0 | 140.0 (s) | 137.5 (s) | 137.5 (s) | 135.0 (s) | 132.5 (s) |
| 12.5 | 127.5 (s) | 127.5 (s) | 127.5 (s) | 125.0 (o) | 122.5 (o) |
| 15.0 | 120.0 (s) | 120.0 (s) | 115.0 (o) | 112.5 (o) | 110.0 (o) |
| 17.5 | 110.0 (s) | 110.0 (o) | 100.0 (o) | 97.5 (o) | 95.0 (o) |
| 20.0 | 100.0 (s) | 95.0 (o) | 87.5 (o) | 82.5 (o) | 82.5 (o) |
| 22.5 | 87.5 (s) | 80.0 (o) | 70.0 (o) | 67.5 (o) | 65.0 (o) |
| 25.0 | 75.0 (s) | 62.5 (o) | 50.0 (o) | 45.0 (o) | 40.0 (o) |

Note: o-Overturning accident; s-Sideslip accident; r-Rotation accident.

stiffness and lighter damper damping, the dominant accident type is the overturning accident. These results indicate that the rigid suspension assumption is not proper for estimating accident vehicle speed and type.

7. Conclusions

The effects of road surface roughness and vehicle suspension on accident vehicle speed/ wind speed of a high-sided road vehicle entering a sharp-edged crosswind have been investigated in detail. This included the modelling of the high-sided road vehicle, the simulation of the random roughness of the road surface, the estimation of crosswind forces on the road vehicle, and the derivation of nonlinear governing equations of motion of the system. The extensive computation results demonstrated that the road surface condition in the vertical direction affected the vertical displacement responses and contact forces of the vehicle but not the lateral and rotational displacement responses of the vehicle. The vehicle suspension affected not only the vertical displacement responses and contact forces but also the lateral and rotational displacement responses of the vehicle. For a given gust wind speed, a better road condition gave a slightly higher accident vehicle speed. However, for a given gust wind speed, a softer suspension system resulted in a lower accident vehicle speed. For the high-sided road vehicle investigated, the overturning type accident was dominant but the sideslip type accident also occurred. The rigid suspension assumption is not proper for estimating accident vehicle speed and type.

It should be pointed out that the above conclusions were drawn based on the high-sided road vehicle and crosswind forces specified in this study. More studies on various types of vehicles and field observations/experiments are needed before general conclusions can be made.

Acknowledgements

The writers wish to acknowledge the financial support from the Research Grants Council of Hong Kong (Project No. PolyU 5043/01E) and the National Natural Science Foundation of China (Project No. 50208019). The writers would also like to express their sincere gratitude to Prof. C.J. Baker from University of Birmingham, UK, for his valuable discussion and useful information.

References

- Baker, C.J. (1986), "A simplified analysis of various types of wind-induced road vehicle accidents", *J. Wind Eng. Ind. Aerodyn.*, **22**, 69-85.
- Baker, C.J. (1987), "Measures to control vehicle movement at exposed sites during windy periods", *J. Wind Eng. Ind. Aerodyn.*, **25**, 151-161.
- Baker, C.J. and Reynolds, S. (1992), "Wind induced accidents of road vehicles", *Accident Analysis and Prevention*, **24**(6), 559-575.
- Chopra, A.G. (1995), *Dynamics of Structures*, Prentice-Hall, Upper Saddle River, New Jersey.
- Coleman, S.A. and Baker, C.J. (1990), "High-sided road vehicle in cross winds", *J. Wind Eng. Ind. Aerodyn.*, **36**, 1383-1392.
- Dodds, C.J. and Robson, J.D. (1973), "The description of road surface roughness", *J. Sound Vib.*, **31**, 175-183.
- Fafard, M., Bennur, M., and Savard, M. (1997), "A general multi-axle vehicle model to study the bridge-vehicle interaction", *Engineering Computations*, **14**, 491-508.
- Guo, W.H. and Xu, Y.L. (2001), "Fully computerized approach to study cable-stayed bridge-vehicle interaction", *J. Sound Vib.*, **248**, 745-761.
- Pritchard, J.R. (1985), "Wind effects on high-sided vehicles", *J. the Institution of Highways and Transportation*, 22-25.
- Wang, T.L. and Huang, D.Z. (1992), "Cable-stayed bridge vibration due to road surface roughness", *J. Struct. Eng., ASCE*, **118**, 1354-1374.

CC